

MODELLING THE SPECTRAL NOISE OF SINGLE AND DOUBLE PASS Er^{3+} -DOPED Ti:LiNbO_3 \mathcal{M} -MODE STRAIGHT WAVEGUIDE AMPLIFIERS

N. N. Puscas

Physics Department, University "Politehnica" of Bucharest,
Splaiul Independentei 313, 77206, Bucharest, Romania

In this paper we present a theoretical analysis of some parameters which characterize the Er^{3+} -doped Ti:LiNbO_3 \mathcal{M} -mode straight waveguides. The derivation and the evaluation of the spectral optical gain, the spectral noise figure, the signal to noise ratio and the amplified spontaneous emission photon number are performed under small gain approximation. The simulations show the evolution of these parameters under various pumping regimes and waveguide lengths. The obtained results can be used for the design of complex integrated circuits with rare earth doped lithium niobate waveguide amplifiers.

(Received September 2, 2002; accepted October 31, 2002)

Keywords: Spectral noise, Erbium doped Ti:LiNbO_3 , Waveguide amplifier

1. Introduction

The study of the spectral noise plays an important role in obtaining integrated amplifiers having low noise and high optical gain. That's why, over the last years, a great attention has been devoted to the analysis of the spectral optical gain and noise of Er doped fibres and waveguide amplifiers [1-7].

In this paper, we propose a novel technique for evaluating the spectral optical gain, the spectral noise figure, the signal to noise ratio and the amplified spontaneous emission (ASE) photon number of \mathcal{M} -mode straight Er^{3+} -doped Ti:LiNbO_3 amplifiers. The reason of this analysis is related to the fact that in waveguides, not only the fundamental mode but also other high order (\mathcal{M}) modes are often excited which, influence the above mentioned parameters and the statistical properties of the waveguide.

The refractive index distribution, as well as the optical mode profile are calculated by means of a conform transformation and an effective index method. Simulations of the gain and noise figure of the amplifier are conducted under small gain approximation for z propagating crystals, pumped near 1484 nm, for various pumping regimes and waveguide lengths. The results thereby computed are compared to those calculated for single mode straight waveguides.

In Section 2 we present the basic equations used to evaluate the population of the upper atomic energy level, and the evolution of the pump signal, ASE gain noise figure, ASE photon number and signal to noise ratio of the \mathcal{M} -mode waveguides. Also, in this section the model used for the calculation of optical field distribution in the waveguide is outlined [8, 9]. Section 3 deals with the discussion of the simulation results, while some conclusions of this work are presented in Section 4.

2. Theoretical considerations

The amplification in straight \mathcal{M} -mode Er^{3+} -doped Ti:LiNbO_3 waveguide amplifiers is described using a quasi-two-level model under the small gain approximation in the wavelength range $1.44 \mu\text{m} < \lambda < 1.64 \mu\text{m}$ [1], [5], [7].

The system of coupled first order differential equations in the case of the two-level model for the upper population level $N_2(x, y, z)$ and the optical power spectral components $P_{km}^\pm(z)$ with the frequency ν_k at the longitudinal coordinate z has the form [7]:

$$\begin{aligned} \frac{d}{dz} P_{km}^\pm(z) = \pm \left\{ \left[(\sigma_{e,km} + \sigma_{a,km}) \int_A N_2(x, y, z) i_{km}(x, y) dx dy \right] P_{km}^\pm(z) \right\} \pm \\ \left\{ - \left[(\sigma_{a,km} \int_A N_T(x, y, z) i_{km}(x, y) dx dy + \alpha_{km}) \right] P_{km}^\pm(z) \right\} \pm \\ \left\{ h\nu_k \Delta\nu_k \sigma_{e,km} \int_A N_2(x, y, z) i_{km}(x, y) dx dy \right\} \end{aligned} \quad (1)$$

where,

$$N_2(x, y, z) = N_{T0} d(x, y) \frac{\sum_{k,m} \frac{\tau}{h\nu_k} \sigma_{a,km} (P_{km}^+(z) + P_{km}^-(z)) i_m(x, y)}{1 + \sum_{k,m} \frac{\tau}{h\nu_k} (\sigma_{a,km} + \sigma_{e,km}) (P_{km}^+(z) + P_{km}^-(z)) i_m(x, y)} \quad (2)$$

The power spectral components, $P_{km}^\pm(z)$ represent the power longitudinal distribution of the field component at frequency ν_k , having the polarization denoted by the index m (m being π for the parallel or σ for the perpendicular directions to the optical axis of the crystal) in the forward (+) and backward (-) propagation directions; the normalized transversal intensity distribution $i_{km}(x, y)$ has been considered wavelength independent. The scattering losses of the integrated optical waveguides have been taken into account by the term α_{km} .

In Eq. (2), the term $h\nu_k \Delta\nu$ represents an equivalent spontaneous emission input noise power in the frequency slot $\Delta\nu$ corresponding to the frequency ν_k . The Er-dopant concentration is

$$N_T(x, y) = N_1(x, y, z) + N_2(x, y, z), \quad (3)$$

where $N_1(x, y, z)$ is the population of the ground state. The dopant concentration can be written in terms of surface concentration N_{T0} and normalised dopant distribution $d(x, y)$. Therefore: $N_T(x, y) = N_{T0} d(x, y)$.

The normalized field transversal intensity distribution can be written as:

$$i(x, y) = \sum_{j=1}^{\mathcal{M}} \eta_j i_j(x, y) \exp[i(\omega t - \beta_j z)] \quad (4)$$

where β_j are the propagation constants which are different for different modes because of their velocity and

$$\eta_j = \frac{\iint E_p(x, y) \cdot E_j(x, y) dx dy}{\sqrt{\iint E_p^2(x, y) dx dy} \sqrt{\iint E_j^2(x, y) dx dy}} \quad (5)$$

are the overlap coefficients between the pump optical field, $E_p(x, y)$ and the mode fields, $E_j(x, y)$ excited in the waveguide, which satisfy a normalization condition $\sum_{j=1}^{\mathcal{M}} \eta_j = 1$.

In our model we considered that the waveguide is pumped by a radiation having a Gaussian distribution of the field using an optical fiber. The integrals in Eq. (5) are extended over the transversal section of the waveguide, x representing the width and y the depth.

In order to determine the optical field distribution in the waveguide we calculated first the refractive index profiles using the Fick's diffusion law [8, 9]. After that, the optical mode fields were calculated numerically for both TE and TM polarisation using the effective index method presented in papers [8, 9]. Figs. 1 a) and b) show the field distribution profile in the case of the lowest four order modes considered in our simulations.

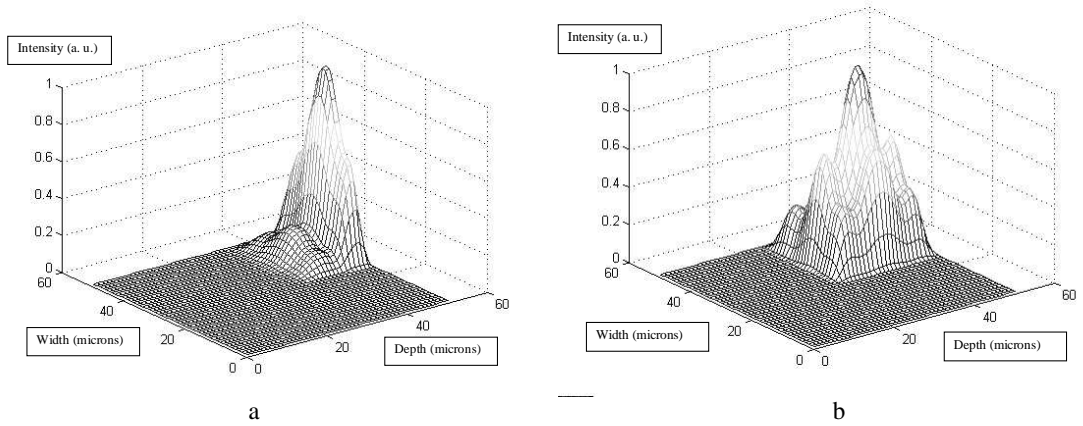


Fig. 1. The normalized field transversal intensity distribution profiles for TE (a) and TM, (b) polarizations, respectively (calculated by the effective index method, for the case of the lowest four order modes).

Using the photon statistics master equation of the linear amplifier and the theoretical model presented in papers [1] and [7] we calculated the photon number mean value $\langle n(z) \rangle$ as:

$$\langle n(z) \rangle = G(z) \langle n(0) \rangle + N(z) \quad (6)$$

where:

$$G(z, \nu) = \exp \left\{ \int_0^z [\gamma_e(z', \nu) - \gamma_a(z', \nu)] dz' \right\} \quad (7)$$

$$N(z, \nu) = G(z, \nu) \int_0^z \frac{\gamma_e(z', \nu)}{G(z', \nu)} dz' \quad (8)$$

represent the gain function and the ASE spectrum at the z section, respectively.

In Eqs. (7)-(8)

$$\gamma_e = \gamma_e(z, \nu) = \sigma_e(\nu) \int_A N_2(x, y, z) i(x, y) dx dy \quad \text{and} \quad \gamma_a = \gamma_a(z, \nu) = \sigma_a(\nu) \int_A N_1(x, y, z) i(x, y) dx dy \quad (9)$$

and the polarization subscript m has been omitted for simplicity.

In deriving Eqs. (6)-(9) we considered that the normalized mode intensity profile $i(x, y)$ in the \mathcal{M} mode straight Er^{3+} -doped Ti:LiNbO_3 waveguide amplifiers is not uniform over its transversal section [7].

Taking into account the relations between the forward $P^+(z) = P^+(0)G(z)$ and backward $P^-(0) = P^-(z)G(z)$ powers we calculated the gain $G(z, \nu)$ and the amplified spontaneous emission noise $N(z, \nu)$ for the single pass (mirror reflectivity in $z=L$, $R_p(L) = R_s(L) = 0$) and the double pass ($R_p(L) = R_s(L) = R$) configuration of the linear amplifier having the length L .

The expressions for the output signal gain are:

$$G(L, \nu) = P_s^+(L) / P_s(0), \quad (10)$$

for the single pass and

$$P_s^-(0) / P_s(0) = G^2(L, \nu) R(L), \quad (11)$$

for the double pass configurations.

Similarly, for the ASE photon number one obtained:

$$N(L, \nu) = G(L, \nu) \int_0^L \frac{\gamma_e(z', \nu)}{G(z', \nu)} dz', \quad (12)$$

for the single pass and

$$N(0, \nu) \cong R(L) G^2(L, \nu) \int_0^L \frac{\gamma_e(z', \nu)}{G(z', \nu)} dz' + \int_0^L \gamma_e(z', \nu) G(z', \nu) dz', \quad (13)$$

for the double pass, respectively assuming that the incident and the reflected fields have the same statistics [1, 7].

The signal to noise ratio, SNR can be defined as follows [1, 7]:

$$SNR_0(z) = \frac{\langle \langle n(z) \rangle - \langle n(z) \rangle_{ASE} \rangle_T^2}{\sigma^2(z)} = G^2(z) n(0) \langle \rangle^2 / \left(\langle G(z) n(0) \rangle + N(z) + 2G(z) N(z) \langle n(0) \rangle + N^2(z) \right) \quad (14)$$

where, $\langle \dots \rangle_T$ represents the time average over the bit period (bit rate $B = 1/T$) and $\sigma^2(z) = \langle n^2(z) \rangle - [\langle n(z) \rangle]^2$, the noise power measured over this period [1].

A measure of the *SNR* degradation experienced by the signal after passing through the amplifier is characterized by the amplifier optical noise figure, $F_0(z)$ defined by the relation:

$$F_0(z) = \frac{SNR_0(0)}{SNR_0(z)} \quad (15)$$

where, $SNR_0(0)$ represents the optical *SNR* at the amplifier input. In the case of large gain (i. e. $G(z) \gg 1$) the noise figure is given by [1]:

$$F_0(z, \nu) = \frac{1 + 2N(z, \nu)}{G(z, \nu)} \quad (16)$$

where the term $2N/G$ corresponds to a beat noise regime at the peak gain and the term $1/G$ to a shot noise at the spectrum tails.

The corresponding equations for *SNR* and noise figure for single and double pass, respectively take the form:

$$SNR(L, \nu) = \frac{\langle n(0) \rangle G(L, \nu)}{1 + 2G(L, \nu) \int_0^L \frac{\gamma_e(z', \nu)}{G(z', \nu)} dz'} \quad (17)$$

$$SNR(L, \nu) = \frac{\langle n(0) \rangle R(L) G^2(L, \nu)}{R(L) G(L, \nu) \left(1 + 2G(L, \nu) \int_0^L \frac{\gamma_e(z', \nu)}{G(z', \nu)} dz' \right) + 1 - G(L, \nu) + 2 \int_0^L \gamma_e(z', \nu) G(z', \nu) dz'} \quad (18)$$

$$F(L, \nu) = \frac{1 + 2G(L, \nu) \int_0^L \frac{\gamma_e(z', \nu)}{G(z', \nu)} dz'}{G(L, \nu)} \quad (19)$$

$$F(L, \nu) = \frac{R(L) G(L, \nu) \left(1 + 2G(L, \nu) \int_0^L \frac{\gamma_e(z', \nu)}{G(z', \nu)} dz' \right) + 1 - G(L, \nu) + 2 \int_0^L \gamma_e(z', \nu) G(z', \nu) dz'}{R(L) G^2(L, \nu)} \quad (20)$$

We considered that the input signals are characterized by Poissons statistics (coherent light), $P_n(0) = \frac{\langle n(0) \rangle^n}{n!} \exp[-\langle n(0) \rangle]$ for which it is well known that $\sigma^2(0) = \langle n(0) \rangle$.

3. Discussion of the simulation results

The system of coupled first order differential equations (1) and (2) can only be solved by numerical methods. We used a Runge-Kutta formula (4-th order, 4 stages) as the basic integration

method with an iterative procedure [7]. In our model, the spontaneous emission spectrum is divided into 100 slots which corresponds to a wavelength resolution, $\Delta\lambda = 2$ nm in the region 1450-1650 nm.

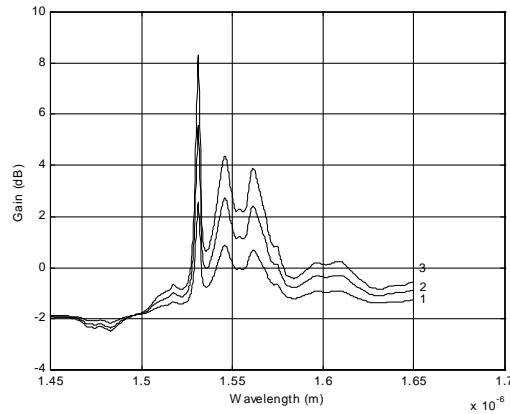


Fig. 2. Spectral behaviour of the double pass gain $G(\mathbf{0}, \nu)$ for the input pumping power of 100 mW in the case of erfc (curve 1), Gaussian (curve 2) and constant (curve 3) dopant profiles in depth, TE polarization and $L=5.4$ cm for the waveguide length.

The lowest four order mode intensity profiles, $i(x, y)$ for both TE and TM polarisations are calculated numerically with the method described in Section 3, while the dopant distribution $d(x, y)$ (with a surface concentration of about $1 \times 10^{26} \text{ m}^{-3}$, a diffusion depth of $20 \mu\text{m}$ and of $5.12 \mu\text{m}$ in width, defined at $1/e$, by an erfc, a Gaussian and a constant function in depth (labelled 1, 2 and 3, respectively), and a Gaussian function in width. These different Er concentration profiles correspond to various diffusion conditions (not complete or complete diffusion, or doping during the crystal growth).

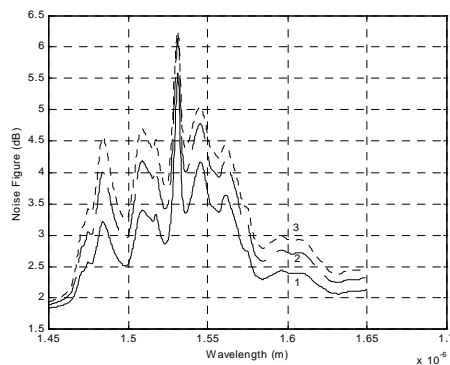


Fig. 3. The noise figure spectra as in Fig. 2.

The computer simulations for the evaluation of the statistical properties of Er^{3+} -doped LiNbO_3 waveguide amplifiers have been performed using the parameters found from literature [5, 7]. We assumed a 1484 nm wavelength pump and a signal at $\lambda = 1531$ nm and $1 \mu\text{W}$ input power. In

computing the profile of the optical modes we used the following characteristic parameters of Ti waveguides: 7 μm for waveguide width, 0.1 μm for Ti thickness, 10 hours for diffusion time [8].

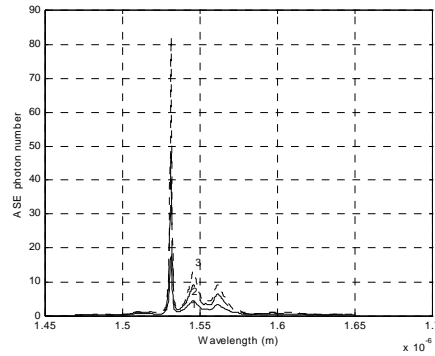


Fig. 4. Spectral behaviour of the ASE photon number in the double pass configuration for input pumping power: $P(0)=100$ mW as in Fig. 2.

In our simulations we used, for TE and TM pump (p) and signal (s) absorption (a) and emission (e) cross sections, the values presented in papers [5], [7]. The waveguide length is assumed to be $L=5.4$ cm. when not specified; the pump and signal input reflectivity, $R(0)=0$, while the output reflectivity, $R(L)=0$ or $R(L)=0.98$ for the single and double pass configuration, respectively. Scattering losses $\alpha=3.7$ dBm⁻¹ for TE, $\alpha=4.8$ dBm⁻¹ for TM and, spontaneous emission lifetime, $\tau=2.6$ ns have been assumed. We limit our presentation to the TE pump and signal polarization; similar results can be obtained for the other cases.

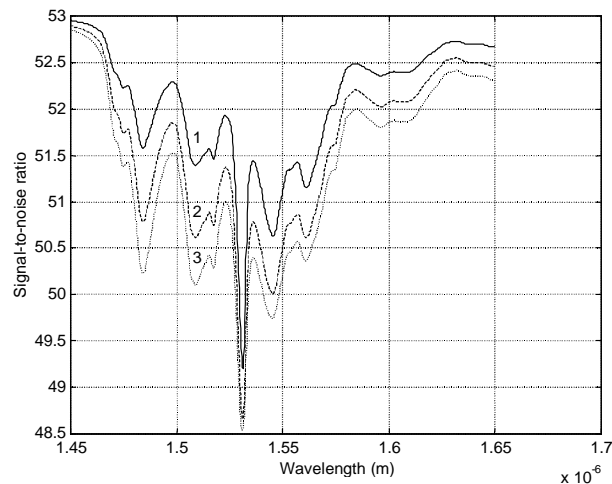


Fig. 5. The SNR spectra in double pass configuration for pumping power $P(0)=100$ mW as in Fig. 2.

The small signal gain $G(z) = \ln[P_{\text{signal}}(z)/P_{\text{signal}}(0)]$ for the double pass configuration, $G(0, \lambda)$ is presented in Fig. 2 for the input pump power of 100 mW (high pumping regime) in the case of erfc, Gaussian and constant dopant profiles in depth and Gaussian in width. The peak values of the gain at $\lambda=1531$ nm for the erfc (2.55 dB), Gaussian (5.57 dB) and constant (8.30) dopant

profiles in the case of \mathcal{M} -mode operation are smaller than in the single one, of about 14.5 dB, quoted for a Gaussian profile in depth [5].

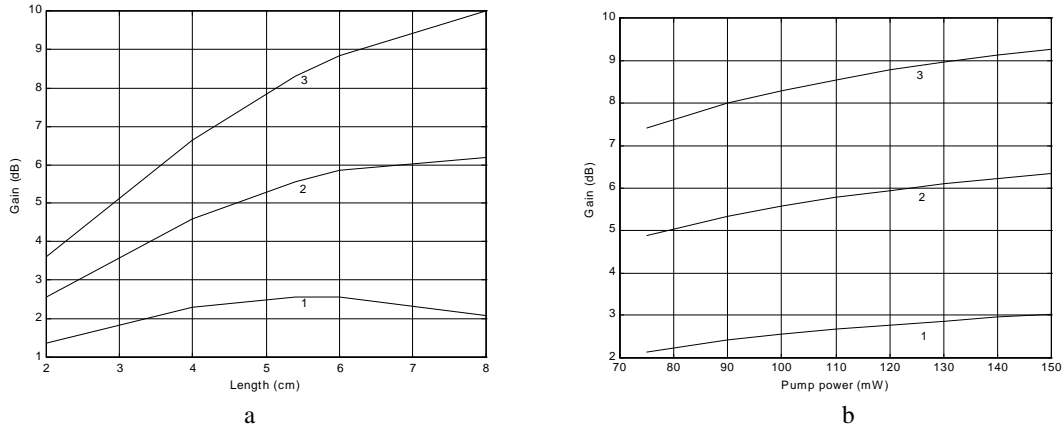


Fig. 6 a), b). The gain in double pass configuration, TE polarization vs the waveguide length for 100 mW pump power and 1 μ W input signal having $\lambda=1531$ nm (a) and vs the input pump power for an amplifier length $L=5.4$ cm (b). Curves labelled 1, 2 and 3, correspond respectively to an Er distribution in erfc function, Gaussian function, and constant functions in width and Gaussian profiles in depth.

The peak values of the noise figure (Eq. (20)) for the erfc (5.58 dB), Gaussian (6.13 dB) and constant (6.24) dopant profiles in the case of \mathcal{M} -mode operation (Fig. 3) are greater than those quoted for the single one, i.e. of about 5.3 dB for Gaussian profile in depth [5].

As can be seen (Figs. (2) and (3)) the behaviour of the gain and noise figure are determined by the absorption and emission cross sections of Er^{3+} -doped LiNbO_3 [5], [7]. In an interval of 2 nm around $\lambda=1531$ nm the double pass configuration with high pump regime ($P(0)=100$ mW) allows us to obtain rather high gains (about 5.57 dB) and low noise figures, (6.13 dB) for an Er^{3+} -doped LiNbO_3 waveguides amplifier of 5.4 cm length.

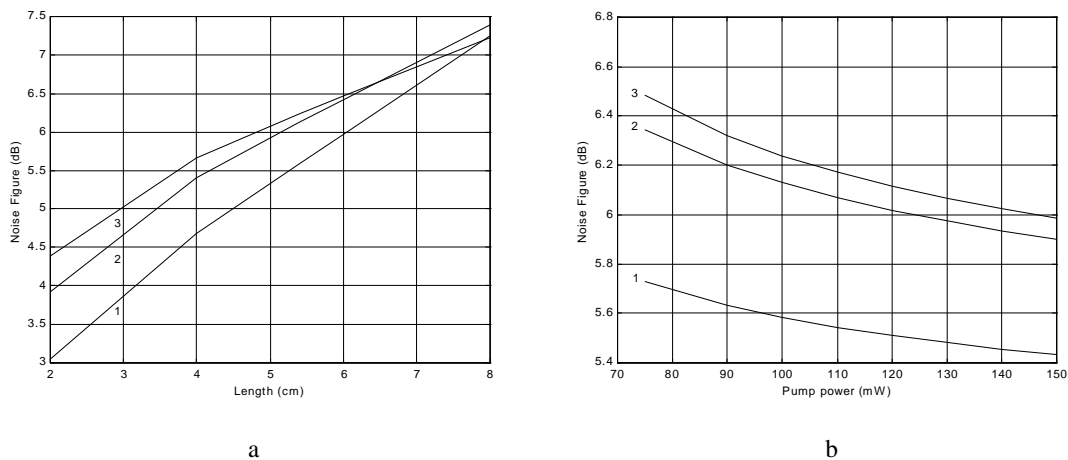


Fig. 7 a), b). The noise figure in double pass configuration, as in Fig. 6.

The \mathcal{M} -mode operation, in comparison with the single one, determines the diminution of the gain and the enhancement of the noise figure because the overlap integral between the population of the excited level and the normalized intensity field profile is smaller in the case of \mathcal{M} -mode operation, compared to that in the case of the single one, (i. e. 1.21 times in the case of Gaussian profile of the dopant for a waveguide having 5.4 cm length and for an input pumping power of 100 mW). Also, the \mathcal{M} -mode operation affects the output statistics by diminishing the coherent properties of the light.

The double pass ASE photon number and SNR spectra are presented in Figs. 4 and 5, in the above mentioned conditions; the spectra show maxima and minima, respectively around 1531 nm.

In Figs. 6 a), b)-8 a), b) the dependence of the gain, noise figure and SNR versus the waveguide length, (a) and respectively the input pumping power, (b) are presented.

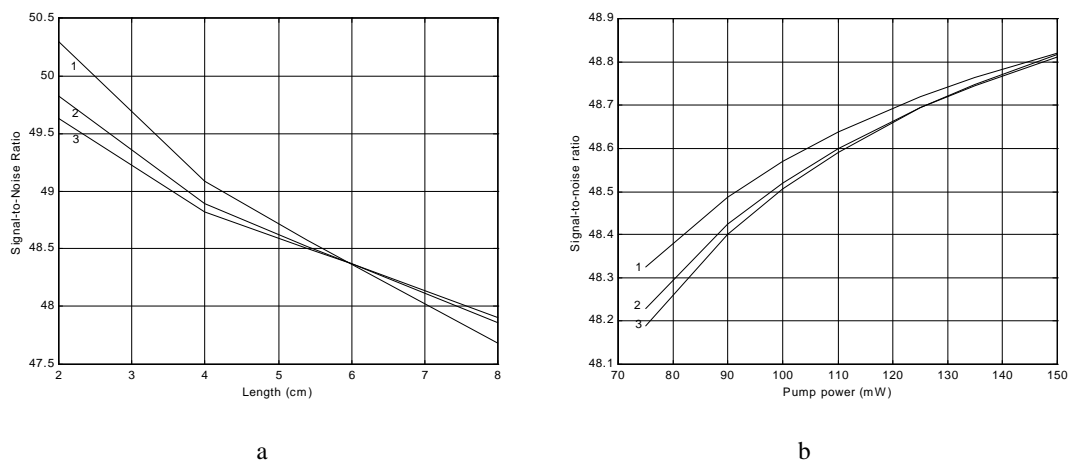


Fig. 8 a), b). The SNR in double pass configuration, as in Fig. 6.

For the Gaussian dopant profile, the gain tends to saturate for waveguide lengths greater than 6 cm, while for erfc profile the gain has a maximum value of about 2.6 dB for a waveguide length of about 5.5 cm (Fig. 6 a). When computing the evolution of the noise figure as a function of the waveguide length in the range 1 - 8 cm for single and double pass configuration we observed that this parameter increases to rather high values (about 7 dB in Fig. 7 b) for the double pass configuration. In the case of a Gaussian profile (for Er-ions), the double pass configuration, waveguide length of 6 cm and for 100 mW pumping power, an increase of the gain of about 2.5 dB and of the noise figure of about 2 dB. However, for an increase of the pumping power from 80 mW to 100 mW and a waveguide length of 5.4 cm gave an increase of the gain of about 0.5 dB and a decrease of the noise figure of about 0.15 dB.

Therefore, it seems that the amplifier length is related to the increase of the noise in the waveguide amplifiers. In the case of shorter waveguide lengths but higher pumping levels, for which the gain reaches rather high values, low values of the noise figure are obtained. This is a consequence which is relevant to the design of complex structures. If the miniaturization of the integrated devices have to be considered, it is preferable to choose short waveguide lengths and high pumping levels, rather than long waveguide and low pumping regimes.

4. Conclusions

In the small gain approximation the spectral optical gain, the spectral noise figure, the signal to noise ratio and the amplified spontaneous emission photon number of a \mathcal{M} -mode Er^{3+} -doped LiNbO_3 straight waveguide amplifier, pumped at 1484 nm in the TE mode have been obtained.

We have shown that the above mentioned parameters are more sensitive to the waveguide length than to the pumping power. The theoretical results of this simulation characterize the Er^{3+} -doped LiNbO_3 waveguide amplifier from the point of view of the gain and noise and can be used for better understanding of the amplification process.

References

- [1] E. Desurvire, *Erbium-Doped Fiber Amplifiers* (New York: Wiley), 1994.
- [2] I. Baumann, S. Bosso, R. Brinkmann, R. Corsini, M. Dinand, A. Greiner, K. Schäfer, J. Söchtig, W. Sohler, H. Suche, R. Wessel, *IEEE J. Selected Topics in Quant. Electron.* **2**, 355 (1996).
- [3] C. H. Huang, L. McCaughan, *IEEE J. Selected Topics in Quant. Electron.* **2**, 367 (1996).
- [4] D. L. Veasey, J. M. Gary, J. Amin, J. A. Aust, *IEEE J. Quant. Electron.* **33**, 1647 (1997).
- [5] M. Dinand, W. Sohler, *IEEE Journal of Quant. Electron.* **30**, 1267 (1994).
- [6] F. Caccavale, F. Segato, I. Mansour, *J. Lightwave Technol.* **15**, 2294 (1997).
- [7] N. N. Puscas, R. Girardi, D. Scarano, I. Montrosset, *J. Mod. Optics* **45**, 847 (1998).
- [8] N. Puscas, B. Wacogne, A. Ducariu, B. Grappe, , *Opt. and Quant. Electron.* **32**, 1 (2000).
- [9] D. Marcuse, *Light Transmission Optics* (New York: Van Nostrand) 1992.